IEEE Access
Multidisciplinary ⋮ Rapid Review ⋮ Open Access Journal

Received December 9, 2020, accepted January 3, 2021, date of publication January 13, 2021, date of current version January 22, 2021.

Digital Object Identifier 10.1109/ACCESS.2021.3051306

Joint Effects of Imperfect CSI and SIC on NOMA Based Satellite-Terrestrial Systems

JINLONG ZHAO[1], XINWEI YUE[2], (Member, IEEE), SHAOLI KANG[1,3], AND WANWEI TANG[4]

[1]School of Electronic and Information Engineering, Beihang University, Beijing 100191, China
[2]School of Information and Communication Engineering, Beijing Information Science and Technology University, Beijing 100101, China
[3]State Key Laboratory of Wireless Mobile Communications, China Academy of Telecommunications Technology (CATT), Beijing 100094, China
[4]Intelligence and Information Engineering College, Tangshan University, Tangshan 063000, China

Corresponding author: Jinlong Zhao (zhaojinlong@buaa.edu.cn)

This work was supported in part by the Natural Science Foundation of Beijing Municipality under Grant 4204099, in part by the Science and Technology Project of Beijing Municipal Education Commission under Grant KM202011232003, in part by the Key Research and Cultivation Project at Beijing Information Science and Technology University under Grant 5211910924, in part by the Supplementary and Supportive Project for Teachers at Beijing Information Science and Technology University under Grant 5111911147, and in part by the Key Research and Innovation Project of Gansu University of Political Science and Law under Grant GZF2020XZD14.

ABSTRACT This paper investigates a satellite-terrestrial system employing the non-orthogonal multiple access (NOMA) scheme over Shadowed-Rician fading channels. The effects of both imperfect channel state information (CSI) and imperfect successive interference cancellation (SIC) on the NOMA based satellite-terrestrial system are taken into account. First, the outage performance of the proposed system is evaluated, and the closed-form expressions for the exact and asymptotic outage probabilities are obtained. Next, the expressions of the ergodic sum rate and system throughput are derived in the presence of channel estimation errors and residual interference. Moreover, we analyze the impacts of different residual interference levels on the energy efficiency. Finally, the numerical simulation results are conducted to verify the correctness of theoretical analysis and the advantages of the proposed NOMA scheme. At medium-high SNR region, the NOMA users are capable of outperforming orthogonal multiple access (OMA) users in terms of outage behaviors and system throughput with imperfect CSI and imperfect SIC. The ergodic sum rate decreases as the level of residual interference ϖ increases, and is even lower than that of OMA once ϖ goes beyond a certain value. Additionally, the energy efficiency of NOMA scheme is sensitive to the imperfect SIC.

INDEX TERMS Satellite-terrestrial system, non-orthogonal multiple access (NOMA), imperfect CSI, imperfect SIC.

I. INTRODUCTION

With the development of wireless mobile communication technology, the satellite-terrestrial network has been widely recognized as an important application scenario for providing users with global services. Due to the spectrum scarcity in spatial information networks and the growth of mobile Internet data, massive connection data has become an important factor restricting the development of satellite communication. Non-orthogonal multiple access (NOMA) serves multiple users on the same time-frequency resource block, which can effectively improve system capacity, spectrum efficiency and meet the technical requirements of large connection [1]–[5]. Therefore, the introduction of NOMA technology into the satellite network has realized an effective management and efficient utilization of resources.

The NOMA based integrated terrestrial-satellite networks were investigated, in which the satellite and NOMA based terrestrial networks cooperatively provided services to ground users [6]. Inspired by the idea of NOMA, a non-orthogonal signature code for different antenna elements was designed to improve the hardware efficiency of large scale satellite antenna arrays [7]. The authors proposed a satellite transmission scheme based on different multibeam in [8] where the NOMA technology was used by terrestrial users. To guarantee user fairness, unmanned aerial vehicles were first integrated into the satellite network adopting NOMA, and then the outage performance under fixed power distribution was analyzed in [9]. The authors in [10] proposed a downlink NOMA-based land mobile satellite network, and analyzed the closed-form expressions of outage probability

The associate editor coordinating the review of this manuscript and approving it for publication was Mohammad S Khan.

and ergodic sum capacity. Moreover, the energy efficiency and average symbol error rate performances were obtained analytically. In order to obtain quasi-optimal performance and balance user fairness, Jia *et al.* [11] constructed the architectures of downlink bandwidth compression NOMA scheme, and presented the receiver design and signal detection scheme in satellite-terrestrial networks. In [12], Lin *et al.* studied an integrated system with a multi-user downlink framework, in which the satellite networks employed NOMA technology to significantly improve the scarce spectrum efficiency and service stability. The authors in [13] investigated the amplify-and-forward relaying assisted cognitive hybrid satellite-terrestrial overlay networks where the closed-form expressions for exact and asymptotic outage probabilities were derived. Based on [13], V. Singh *et al.* designed an overlay scheme integrating the secondary ground relay cooperatively into primary direct satellite communication to achieve diversity gain in primary networks [14]. Taken into account of the wide coverage of satellites and the vulnerability of communications processes to security threats, the work in [15] proposed a frequency-domain non-orthogonal multiple access scheme and studied the physical layer security of satellite downlink. In addition, to take full advantage of the multi-antenna technology in the terrestrial-satellite networks, the authors in [16] investigated the outage performance of a multiuser dual-hop satellite relaying system with threshold-based decode-and-forward protocol, where the relaying satellite exploited the point-beam scheme to assist the terrestrial multi-antenna users. In order to maximize the ergodic capacity of terrestrial users, a virtual uplink based transmit beamforming algorithm was investigated in a hybrid satellite-terrestrial system [17].

In the real communication scenario, due to the combined influence of path loss, channel fading and power attenuation, it is very difficult to obtain perfect channel state information (CSI) [18]. In this case, it is necessary to study the impact of channel estimation error on system performance. Li *et al.* in [18] analyzed the performance of NOMA simultaneous wireless information and power transfer relaying networks over Weibull fading channels, where the imperfect CSI and residual hardware impairments were taken into account. The authors in [19] proposed the NOMA based integrated satellite-terrestrial networks, and studied the effect of impefect CSI on channel estimation by using pilot based channel estimation method. Finally, the validity of the theoretical results were verified by Monte-Carlo simulation. In [20], a genetic optimization algorithm based on NOMA downlink satellite networks was designed, in which NOMA users were selected according to the results of support vector machine classifier.

In addition, due to some potential implementation problems with successive interference cancellation (SIC) decoding, the assumption of perfect SIC may be invalid in practical application scenarios [21]. Therefore, it is of great significance to investigate the effect of imperfect SIC on NOMA strategy. In [22], the performance of full-duplex cooperative NOMA relaying system was studied with in-phase and quadrature-phase imbalance and imperfect SIC, in which the outage probability expressions for both far and near users were derived. The interference from the primary source and the interference constraint of the primary users were analyzed in [23], and the exact outage probability and asymptotic expressions for the secondary users were calculated. Yue *et al.* studied the application of NOMA technology in the satellite communication system and discussed the effect of imperfect SIC on the performance of the proposed system [24].

Although the aforementioned works such as [19], [20] have greatly improved our understanding on the NOMA based terrestrial-satellite networks under imperfect CSI condition, it should be noted that they did not take into account the effect of non-ideal SIC on system performance, and the channels considered were unordered. Additionally, unlike in [24], where the authors assumed perfect channel estimation, we consider the practical scenario where channel estimation is imperfect. These observations inspire the work of this paper. In this paper, we investigate the performance of NOMA based satellite-terrestrial system with imperfect CSI and imperfect SIC under Shadowed-Rician fading channels. The detailed contributions of this paper are summarised as follows:

1) We study the outage behavior of the proposed system and acquire the exact closed-form expressions for the outage probability on the condition of imperfect CSI and SIC. In order to get more insights, the asymptotic outage behavior is derived in the high SNR region. In addition, the influence of satellite channel parameters on system performance is considered.
2) We investigate the ergodic sum rate and system throughput of the NOMA based satellite-terrestrial system, and the effects of channel estimation error and residual interference on sum rate and system throughput are analyzed. Moreover, we discuss the energy efficiency in delay-limited and delay-tolerant transmission modes respectively.
3) Numerical simulation verifies our analysis results and the advantages of the satellite-terrestrial system employing the NOMA scheme. Moreover, the channel estimation error and residual interference can affect the system performance in terms of outage probability, ergodic rate, sum throughput and energy efficiency.

The rest of this article is organized as follows. In Section II, a NOMA based downlink satellite-terrestrial network is introduced and instantaneous SINR is derived. The exact and asymptotic outage performance for the ordered terrestrial users are analyzed in Section III. Then in Section IV, the ergodic rate of satellite-terrestrial NOMA networks is studied. Section V analyzes the sum throughput and energy efficiency of the proposed system. In Section VI, the correctness of the theoretical analysis is verified by numerical simulation. Finally, this paper is summarized in Section VII.

The main notations for this paper are shown below: $F_X(\cdot)$ and $f_X(\cdot)$ represent the cumulative distribution

function (CDF) and the probability density function (PDF) of a random variable X, respectively; $\mathbb{E}\{\cdot\}$ denotes the expectation operator.

II. SYSTEM MODEL

Consider a downlink satellite-terrestrial system where a satellite (S) serves N terrestrial users adopting the NOMA scheme. These N users are randomly deployed within the coverage area of S. All nodes in the considered system are equipped with single antenna, and all the links are subject to Shadowed-Rician distribution. The channel coefficient between S and terrestrial UE_k is denoted by h_k. However, due to the channel estimation error in practical wireless communication system, the channel coefficient h_k estimated at UE_k employing minimum mean squared error can be modeled as $h_k = \bar{h}_k + e_k$, where e_k denotes the estimated channel error with $e_k \sim \mathcal{CN}\left(0, \sigma_{e_k}^2\right)$.

In the proposed system, S transmits a superposed signal to terrestrial users. The received signal at UE_k can be represented as

$$y_k = \left(\bar{h}_k + e_k\right)\sqrt{G_s G_k\left(\psi_k\right)\chi_k a_k P_s}x_k + \underbrace{\left(\bar{h}_k + e_k\right)\sum_{i\neq k}\sqrt{G_s G_k\left(\psi_k\right)\chi_k a_i P_s}x_i}_{\text{Internal-users interference}} + n_k, \quad (1)$$

where G_S denotes the satellite antenna gain, P_S denotes the transmission power at S, x_k is the transmitted message intended for UE_k normalised as $\mathbb{E}\left(|x_k|^2\right) = 1$, and n_k denotes the independent additive white Gaussian noise with the power density σ^2. $G_k\left(\psi_k\right)$ is the antenna gain of UE_k, which is determined by the satellite beam pattern and the position of UE_k. We can obtain $G_k\left(\psi_k\right) = G_k\left(J_1\left(u_k\right)/2\,u_k + 36\,J_3\left(u_k\right)/u_k^3\right)$ in [25] and $u_k = 2.07123\sin\psi_k/\sin\psi_{k3\text{dB}}$. $\psi_{k3\text{dB}}$ denotes the 3 dB angle between UE_k and the beam center with respect to the satellite and $J_\zeta(\cdot)$ is the first-kind Bessel function with order ζ, $\zeta = \{1, 3\}$. In addition, $\chi_k = (c/4\pi f_k d_k)^2$ denotes the free space loss, where c stands for speed of light, f_k is the operating frequency and d_k is the distance between S and the UE_k. a_i represents the power allocation coefficients for UE_i and $\sum_{i=1}^{N} a_i = 1$. Note that the fixed power allocation coefficients for NOMA users are considered. Optimizing the power allocation coefficient will further improve the performance of systems and will be implemented in our future work.

The Shadowed-Rician distribution is determined by three parameters, i.e., the average power of line-of-sight component Ω_k, the average power of the scatter $2b_k$ and the shape parameter of Nakagami-m m_k ($m_k > 0$). Mathematically, the PDF and CDF of $\left|\bar{h}_k\right|^2$ can be expressed as [26]

$$f_{\left|\bar{h}_k\right|^2}(x) = \alpha_k e^{-\beta_k x}\,{}_1F_1\left(m_k; 1; \delta_k x\right) \quad (2)$$

and

$$F_{\left|\bar{h}_k\right|^2}(x) = \alpha_k \sum_{i=0}^{\infty}\frac{(m_k)_i\,\delta_k^i}{(i!)^2\,\beta_k^{i+1}}\gamma\left(i+1, \beta_k x\right) \quad (3)$$

where $\alpha_k = (2\,b_k m_k)^{m_k}/\left(2\,b_k\left(2\,b_k m_k + \Omega_k\right)^{m_k}\right)$, $\beta_k = 1/(2\,b_k)$, $\delta_k = \Omega_k/\left(2\,b_k\left(2\,b_k m_k + \Omega_k\right)\right)$, $(\cdot)_j$ denotes the Pochhammer symbol [27, p. xliii]. $\gamma(a, x) = \int_0^x e^{-t}t^{a-1}dt$ represents the incomplete Gamma function [27, eq.(8.350.1)] and ${}_1F_1(a; b; c)$ represents the confluent hypergeometric function [27, eq.(9.100)].

When decoding at users, SIC will be executed at each user to separate superimposed signals and eliminate the internal-users interference. Moreover, the users are ordered by their estimated channel gain as $\left|\bar{h}_1\right|^2 \leq \left|\bar{h}_2\right|^2 \leq \cdots \leq \left|\bar{h}_N\right|^2$, and the power is allocated to users in the opposite order with $a_1 \geq a_2 \geq \cdots \geq a_N$. Therefore, the SIC decoding sequence is set to $\{1, 2, \cdots, N\}$. Assuming $l < k$, then UE_k should decode firstly the signals of UE_l and subtract its component from his received signals y_k. Due to the effect of imperfect SIC, the residual interference signal from UE_{l-1} is regarded as interfering information. For mathematical tractability, we define $\gamma = P_S/\sigma^2$ as the transmit SNR. Then the SINR for the UE_k to decode the signal of UE_l can be expressed as

$$\Gamma_{k\to l} = \frac{\rho_k a_l \gamma X_k}{\tilde{a}_l \rho_k \gamma X_k + \varpi a_{l-1}\rho_k\gamma X_k + \rho_k\gamma\sigma_{e_k}^2 + 1} \quad (4)$$

where $\rho_k = G_s G_k\left(\psi_k\right)\chi_k$, $\tilde{a}_l = \sum_{i=l+1}^{N} a_i$ for $l < N$, $\tilde{a}_N = 0$ and the channel gain $X_k = \left|\bar{h}_k\right|^2$. ϖ denotes the level of residual interference from UE_{l-1} and $0 \leq \varpi \leq 1$. This SIC will be executed until the messages for k users are all decoded, where the SINR for the k-th user to decode its own signal can be expressed as

$$\Gamma_k = \frac{\rho_k a_k \gamma X_k}{\tilde{a}_k \rho_k \gamma X_k + \varpi a_{k-1}\rho_k\gamma X_k + \rho_k\gamma\sigma_{e_k}^2 + 1} \quad (5)$$

For UE_N, all the other users' signals should be detected first, the received SINR for UE_N to decode its own signal can be expressed as

$$\Gamma_N = \frac{\rho_N a_N \gamma X_N}{\varpi a_{N-1}\rho_N\gamma X_N + \rho_N\gamma\sigma_{e_N}^2 + 1} \quad (6)$$

where the channel gain $X_N = \left|\bar{h}_N\right|^2$.

Due to the same power transmission of L training symbols for CSI estimation, the variance of estimated channel error can be modeled as $\sigma_{e_k}^2 = 1/(\rho_k\gamma L)$.

III. OUTAGE PROBABILITY

In this section, we investigate the outage performance for the NOMA based satellite networks with imperfect CSI and SIC. To guarantee satisfactory quality-of-service (QoS), the data rates of terrestrial users must be higher than predefined target data rates. The outage event occurs when the transmission rate determined by the CSI condition is lower than the target rate [2]. Let us assume that γ_{th_k} and R_k represent the target SINR thresholds and the target rate for UE_k, respectively, and that $R_k = \log\left(1 + \gamma_{th_k}\right)$.

A. EXACT OUTAGE PROBABILITY

The outage event at UE_k is defined as UE_k fails to decode its own signal or the signal of UE_l, $1 \le l \le k$. The event that UE_k correctly decodes the signal of l-th user can be represented as

$$\begin{aligned}\Xi_{k,l} &= \{\frac{\rho_k a_l \gamma X_k}{\tilde{a}_l \rho_k \gamma X_k + \varpi a_{l-1} \rho_k \gamma X_k + \rho_k \gamma \sigma_{e_k}^2 + 1} > \gamma_{th_l}\} \\ &\overset{\text{(i)}}{=} \{X_k > \frac{\gamma_{th_l} \theta_k \left(1 + 1/L\right)}{a_l - \gamma_{th_l} \tilde{a}_l - \varpi \gamma_{th_l} a_{l-1}}\}\end{aligned} \tag{7}$$

where $\theta_k = 1/\rho_k \gamma$ and step (i) satisfies the condition $a_l > \gamma_{th_l}\left(\tilde{a}_l + \varpi a_{l-1}\right)$. If the condition is not satisfied, UE_k can never decode the information of UE_l successfully regardless of the transmit SNR. Therefore, the outage probability for UE_k can be represented as

$$P_{out}^k = 1 - P_r\left(\Xi_{k,1} \cap \Xi_{k,2} \cap \cdots \cap \Xi_{k,k}\right) \tag{8}$$

With the aid of order statistics [28] and binomial theorem, the PDF and CDF of the ordered channel gain X_k can be expressed as

$$\begin{aligned}f_{X_k^{or}}(x) = \frac{N!}{(k-1)!\,(N-k)!} f_{X_k}(x) \left(F_{X_k}(x)\right)^{k-1} \\ \times \left(1 - F_{X_k}(x)\right)^{N-k}\end{aligned} \tag{9}$$

and

$$F_{X_k^{or}}(x) = \frac{N!}{(k-1)!(N-k)!} \sum_{j=0}^{N-k} \binom{N-k}{j} \frac{(-1)^j}{k+j} F_{X_k}^{k+j}(x) \tag{10}$$

respectively. In what follows, we focus on calculating the closed-form expression for the outage probability of UE_k under the imperfect CSI and imperfect SIC conditions. Let

$$\begin{aligned}\phi_k = \max\{&\frac{\gamma_{th_1}\theta_1\left(1+1/L\right)}{a_1 - \gamma_{th_1}\tilde{a}_1}, \frac{\gamma_{th_2}\theta_2\left(1+1/L\right)}{a_2 - \gamma_{th_2}\tilde{a}_2 - \varpi\gamma_{th_l}a_1}, \\ &\cdots, \frac{\gamma_{th_k}\theta_k\left(1+1/L\right)}{a_k - \gamma_{th_k}\tilde{a}_k - \varpi\gamma_{th_k}a_{k-1}}\}\end{aligned} \tag{11}$$

For the convenience of calculations, we assume that m_k takes arbitrary integer values, and the CDF of X_k is given by [29]

$$\begin{aligned}F_{X_k}(x) = 1 - \alpha_k \sum_{s=0}^{m_k-1} \frac{(-1)^s (1-m_k)_s \delta_k^s}{s!} \\ \times \sum_{d=0}^{s} \frac{(\beta_k - \delta_k)^{-(s+1-d)}}{d!} x^d e^{-(\beta_k - \delta_k)x}\end{aligned} \tag{12}$$

Substituting (12) into (10) and combining (4), (5), (6), (8) and (11), the outage probability of UE_k can be calculated as

$$\begin{aligned}P_{out}^k &= 1 - Pr\left(X_k > \phi_k\right) \\ &\overset{\text{(ii)}}{=} \frac{N!}{(k-1)!\,(N-k)!} \sum_{j=0}^{N-k} \binom{N-k}{j} \frac{(-1)^j \alpha_k^{k+j}}{k+j} \\ &\times \left(1 - \alpha_k \sum_{s=0}^{m_k-1} \frac{(-1)^s (1-m_k)_s \delta_k^s}{s!}\right. \\ &\left. \times \sum_{d=0}^{s} \frac{(\beta_k - \delta_k)^{-(s+1-d)}}{d!} \phi_k^d e^{-(\beta_k - \delta_k)\phi_k}\right)^{k+j}\end{aligned} \tag{13}$$

where step (ii) is derived from (10).

B. ASYMPTOTIC OUTAGE PROBABILITY

To get further insights and evaluate the achievable diversity order, we focus on the analysis of asymptotic outage probability for UE_k in the high SNR region. $\gamma\left(i+1, \beta_k\phi_k\right)$ can be expressed as $\gamma\left(i+1, \beta_k\phi_k\right) = \sum_{n=0}^{\infty} \frac{(-1)^n (\beta_k\phi_k)^{n+i+1}}{n!(n+i+1)}$, which is derived from [27, eq.(8.354.1)]. When $\gamma \to \infty$, $\gamma\left(i+1, \beta_k\phi_k\right)$ can be rewritten as

$$\begin{aligned}\gamma_\infty\left(i+1, \beta_k\phi_k\right) &= \lim_{\phi_k \to \infty} \sum_{n=0}^{\infty} \frac{(-1)^n (\beta_k\phi_k)^{n+i+1}}{n!\,(n+i+1)} \\ &\approx \frac{(\beta_k\phi_k)^{i+1}}{i+1}\end{aligned} \tag{14}$$

By plugging (14) into (3) and combining (10), the approximate expression of P_{out}^k can be given by

$$\begin{aligned}P_{out}^{k,asy} = \frac{N!}{(k-1)!(N-k)!} \sum_{j=0}^{N-k} \binom{N-k}{j} \frac{(-1)^j}{k+j} \\ \times \left(\alpha_k \sum_{i=0}^{\infty} \frac{(m_k)_i \delta_k^i}{(i!)^2 \beta_k^{i+1}} \frac{(\beta_k\phi_k)^{i+1}}{i+1}\right)^{k+j}\end{aligned} \tag{15}$$

As a further development, according to [21, eq.(26)] and taking the first term ($i = 0$ and $j = 0$) of (15), the asymptotic outage probability of UE_k can be formulated as

$$P_{out}^{k,asy} = \frac{N!}{k!\,(N-k)!} \left(\alpha_k\phi_k\right)^{k+j} \tag{16}$$

IV. ERGODIC SUM RATE

In this section, taking into account the effect of users' channel condition on the target rate, the ergodic rate of NOMA based satellite-terrestrial system is studied. It is obvious that $\Gamma_{k\to k} = \Gamma_k$ and $R_{k\to k} = R_k$ from (4) and (5). Therefore, the achievable rate of UE_k is expressed as $R_k = \log\left(1 + \Gamma_k\right)$ under the conditions of $\Gamma_{k\to l} > \gamma_{th_l}$ and $l < k$. The ergodic sum rate can be written as (17), shown at the bottom of the next page.

In (17), we note that $\varpi a_{k-1}\rho_k\gamma X_k = 0$ when $k = 1$, and $\tilde{a}_k\rho_k\gamma X_k = 0$ when $k = N$. Next, we start analyzing R_k^{erg}, which represents the achievable rate of UE_k. Through some mathematical computation, R_k^{erg} can be expressed as (18), shown at the bottom of the next page.

To evaluate (18), Φ_1 can be calculated in terms of the PDF as

$$\Phi_1 = \frac{1}{\ln 2} \int_0^\infty \ln\left(1 + \frac{1 + \varpi a_{k-1}}{\theta_k\left(1 + 1/L\right)} X_k\right) f_{X_k^{or}}(x)\, dx \tag{19}$$

With the help of [30, eq.(11)] and [27, eq.(9.34.8)], we express $\ln(1+x)$ in the form of Meijer-G function and ${}_1F_1\left(m_k; 1; \delta_k x\right)$ in (2) as

$$\ln(1+x) = G_{2,2}^{1,2}\left[x \,\middle|\, \begin{matrix} 1, & 1 \\ 1, & 0 \end{matrix}\right] \tag{20}$$

and

$$ {}_1F_1\left(m_k;1;\delta_k x\right)=\frac{1}{\Gamma\left(m_k\right)}G_{1,2}^{1,1}\left[-\delta_k x\,\middle|\,\begin{matrix}1-m_k\\0,\quad 0\end{matrix}\right] \tag{21}$$

respectively, where $G_{2,2}^{1,2}$ and $G_{1,2}^{1,1}$ denote the Meijer-G function of one variable [27, eq.(9.301)]. Due to the complexity of integration, it is difficult to obtain the expression of the rate under the ordered channel gain condition. Hence, we approximate (9) with high SNR. With the aid of [19, eq.(16)], the approximate expression of PDF for the channel gain X_k can be rewritten as

$$ f_{X_k^*}\left(x\right)=\frac{N!}{(k-1)!\,(N-k)!}\sum_{r=0}^{N-k}\binom{N-k}{r}\left(-1\right)^r\alpha_k^{k+r} \times e^{-\beta_k x}x^{k+r-1}\,{}_1F_1\left(m_k;1;\delta_k x\right) \tag{22}$$

To proceed forward, by combining (20), (21) and (22), Φ_1 can be expressed as

$$ \Phi_1=\frac{\Xi_k}{\Gamma\left(m_k\right)\ln 2}\sum_{r=0}^{N-k}\binom{N-k}{r}\left(-1\right)^r\alpha_k^{k+r}\beta_k^{-k-r} \times G_{1,[1:2],0,[2:2]}^{1,1,2,1,1}\left[\begin{matrix}\dfrac{-\delta_k}{\beta_k}\\[2mm]\dfrac{\Lambda_k}{\beta_k}\end{matrix}\,\middle|\,\begin{matrix}(k+r,1)\\(1-m_k);(1,1)\\-\\(0,0);(1,0)\end{matrix}\right] \tag{23}$$

where $\Lambda_k=\frac{1+\varpi a_{k-1}}{\theta_k(1+1/L)}$, $\Xi_k=\frac{N!}{(k-1)!(N-k)!}$ and $G_{1,[1:2],0,[2:2]}^{1,1,2,1,1}$ represents the Meijer-G function of two variables [31].

Proof: See Appendix.

Next, we concentrate on analysing Φ_2. According to the calculation procedure similar to Φ_1, Φ_2 can be derived as

$$ \Phi_2=\frac{\Xi_k}{\Gamma\left(m_k\right)\ln 2}\sum_{s=0}^{N-k}\binom{N-k}{s}\left(-1\right)^s\alpha_k^{k+s}\beta_k^{-k-s} \times G_{1,[1:2],0,[2:2]}^{1,1,2,1,1}\left[\begin{matrix}\dfrac{-\delta_k}{\beta_k}\\[2mm]\dfrac{\Theta_k}{\beta_k}\end{matrix}\,\middle|\,\begin{matrix}(k+s,1)\\(1-m_k);(1,1)\\-\\(0,0);(1,0)\end{matrix}\right] \tag{24}$$

where $\Theta_k=\frac{\tilde{a}_k+\varpi a_{k-1}}{\theta_k(1+1/L)}$.

By plugging (23) and (24) into (18), the ergodic rate of UE_k can be expressed as (see (25), as shown at the bottom of the page). Finally, by substituting (25) into (17), the ergodic sum rate can be obtained.

V. THROUGHPUT AND ENERGY EFFICIENCY ANALYSIS

A. THROUGHPUT ANALYSIS

System throughput is one of the important metrics to evaluate system performance. In this subsection, we consider the delay-limited transmission mode for NOMA based satellite-terrestrial networks, in which the base station transmits information to the users at a fixed rate and the throughput is affected by the wireless fading channels [32]. The sum throughput of the NOMA based satellite-terrestrial system is expressed as

$$ R_{sum}^{l}=\sum_{k=1}^{N}\left(1-P_{out}^{k}\right)\times R_k \tag{26}$$

where P_{out}^{k} can be obtained from (13).

$$ R_{sum}^{t}=\sum_{k=1}^{N}\mathbb{E}\left[\log\left(1+\frac{\rho_k a_k\gamma X_k}{\tilde{a}_k\rho_k\gamma X_k+\varpi a_{k-1}\rho_k\gamma X_k+\rho_k\gamma\sigma_{e_k}^2+1}\right)\right]=\sum_{k=1}^{N}R_k^{erg} \tag{17}$$

$$ R_k^{erg}=\underbrace{\mathbb{E}\left[\log\left(1+\frac{1+\varpi a_{k-1}}{\theta_k\left(1+1/L\right)}X_k\right)\right]}_{\Phi_1}-\underbrace{\mathbb{E}\left[\log\left(1+\frac{\tilde{a}_k+\varpi a_{k-1}}{\theta_k\left(1+1/L\right)}X_k\right)\right]}_{\Phi_2}=\Phi_1-\Phi_2 \tag{18}$$

$$ R_k^{erg}=\frac{\Xi_k}{\Gamma\left(m_k\right)\ln 2}\sum_{r=0}^{N-k}\binom{N-k}{r}\left(-1\right)^r\alpha_k^{k+r}\beta_k^{-k-s}G_{1,[1:2],0,[2:2]}^{1,1,2,1,1}\left[\begin{matrix}\dfrac{-\delta_k}{\beta_k}\\[2mm]\dfrac{\Lambda_k}{\beta_k}\end{matrix}\,\middle|\,\begin{matrix}(k+r,1)\\(1-m_k);(1,1)\\-\\(0,0);(1,0)\end{matrix}\right] -\frac{\Xi_k}{\Gamma\left(m_k\right)\ln 2}\sum_{s=0}^{N-k}\binom{N-k}{s}\left(-1\right)^s\alpha_k^{k+s}\beta_k^{-k-s}G_{1,[1:2],0,[2:2]}^{1,1,2,1,1}\left[\begin{matrix}\dfrac{-\delta_k}{\beta_k}\\[2mm]\dfrac{\Theta_k}{\beta_k}\end{matrix}\,\middle|\,\begin{matrix}(k+s,1)\\(1-m_k);(1,1)\\-\\(0,0);(1,0)\end{matrix}\right] \tag{25}$$

B. ENERGY EFFICIENCY

In satellite network, energy efficiency is another important metric to measure the performance of satellite communication system due to the characteristics of satellite-terrestrial link and the limitation of satellite load. In addition, the satellites are generally powered by solar cells to provide communication services for terrestrial users. By analyzing energy efficiency, power resources can be fully utilized and the battery life can be effectively improved so as to reduce the operating cost of the satellite system. Hence, the energy efficiency of the NOMA based satellite system is investigated in this subsection. Based on the preceding ergodic rate and sum throughput, the energy efficiency of the proposed system can be expressed as [10]

$$\eta_E = \frac{R_\Delta}{\varepsilon P_S + P_L} \tag{27}$$

where $R_\Delta = \{R^t_{sum}, R^l_{sum}\}$ represent the sum rates in delay-tolerant transmission mode and delay-limited transmission mode respectively, and they can be obtained by (17) and (26) respectively. P_L represents the fixed power loss of the satellite communication system and ε is the power amplification factor.

VI. NUMERICAL RESULTS

In this section, we investigate the performance of the proposed NOMA based satellite-terrestrial system under the impact of imperfect CSI and SIC. We assume that the channel links from satellite to the terrestrial users are subject to Shadowed-Rician fading. The channel parameters are referred to [14], [26], and the relevant channel parameters are given in Table 1. In our simulations, we set that the orbit type of satellite is low earth orbit and the number of terrestrial users $N = 3$. Moreover, the carrier frequency is set to 1 GHz, $G_S = 24.3$ dBi, $G_1 = G_2 = G_3 = 3.5$ dBi, $\psi_{k3\text{dB}} = 0.4°$, and the distance between the satellite and terrestrial user is 1000 km. The initial angles between the satellite beam center and the users are set as $\psi_1 = 0.5°$, $\psi_2 = 0.3°$ and $\psi_3 = 0.1°$. Moreover, the power allocation coefficients for multiple users are $a_1 = 0.6$, $a_2 = 0.3$ and $a_3 = 0.1$, and the corresponding target rates are $R_1 = 0.1$ bits/s/Hz, $R_2 = 0.5$ bits/s/Hz and $R_3 = 1.0$ bits/s/Hz, respectively.

TABLE 1. The table of Shadowed-Rician fading channel parameters.

Shadowing Condition	b_k	m_k	Ω_k
Heavy shadowing (HS)	0.063	2	0.0005
Average shadowing (AS)	0.251	5	0.279

Fig. 1 shows the impacts of the transmit SNR and different levels of residual interference signal on the outage probability of the proposed system, where the satellite links undergo AS. It can be seen that exact analytical results agree well with the numerical simulations and the outage probabilities of terrestrial users decrease with the increase of transmit SNR. In addition, the curves of asymptotic outage probability are extremely close to the curves of exact analytical

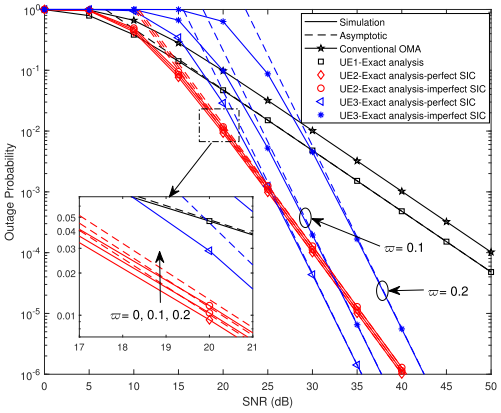

FIGURE 1. Outage probability versus the transmit SNR, with perfect SIC/imperfect SIC and $\varpi = \{0, 0.1, 0.2\}$.

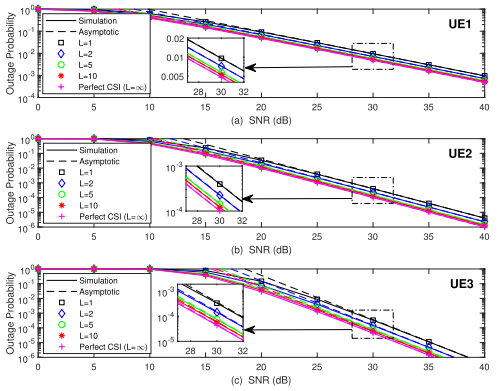

FIGURE 2. Outage probability versus the transmit SNR for various length of training symbols: (a) UE_1, (b) UE_2 and (c) UE_3.

results in the high SNR region. In order to analyze the effect of imperfect SIC on the outage probability, three different levels of residual interference signal $\varpi = \{0, 0.1, 0.2\}$ are focused. Apparently, the outage performance for UE_2 and UE_3 decrease significantly as the level of residual interference increases from 0 to 0.2. Another important observation is that the outage performance of UE_3 is worse than that of UE_1 and UE_1, and even worse than that of conventional orthogonal user in the low SNR region. In this region, UE_3 can easily eliminate x_1 and x_2 due to the high power allocation coefficients of UE_1 and UE_2. However, UE_3 faces difficulties in decoding its own signal because the x_3 has a very low SNR and power allocation coefficient. Finally, it can be seen that NOMA users are capable of exceeding the orthogonal user in terms of outage behaviors with imperfect SIC in medium-high SNR region. This verifies that NOMA can serve multiple users simultaneously, offering better spectrum efficiency and user fairness.

Fig. 2 illustrates the outage probability versus the transmit SNR with different estimation error terms of CSI, where the lengths of training symbols $L = \{1, 2, 5, 10, \infty\}$. For comparison purposes, we adopt the curves of outage probability under perfect channel estimation ($L = \infty$) as counterparts. Apparently, as the length of pilot symbol increases, the outage performance gets better and approaches the perfect CSI

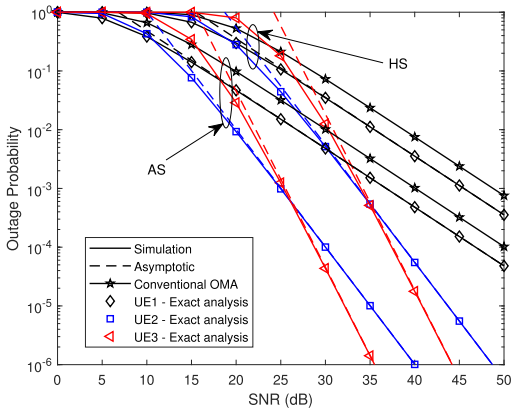

FIGURE 3. Outage probability versus the transmit SNR for various satellite shadowing conditions.

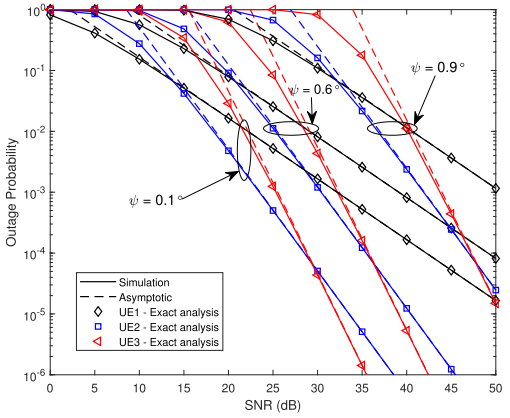

FIGURE 4. Outage probability versus the transmit SNR, with $\psi = \psi_1 = \psi_2 = \psi_3 = \{0.1°, 0.6°, 0.9°\}$.

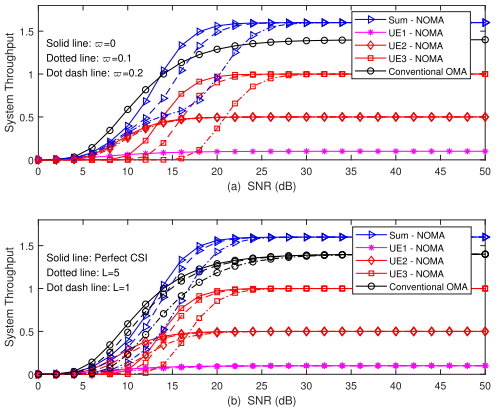

FIGURE 5. System throughput in delay-limited transmission mode versus the transmit SNR, with (a) perfect/imperfect SIC and (b) perfect/imperfect CSI.

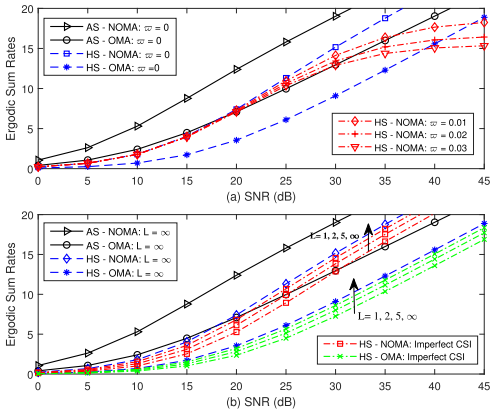

FIGURE 6. Ergodic rates versus the transmit SNR, with (a) perfect/imperfect SIC and (b) perfect/imperfect CSI.

condition gradually. In addition, we have observed that the outage performance increments for terrestrial users become smaller and smaller once L is larger than 5. This means that we can increase the length of training symbols to reduce the impact of channel estimation error on system performance in practical applications.

In Fig. 3, the outage probabilities of terrestrial users versus the transmit SNR are presented in different satellite fading conditions. Obviously, the outage performance is closely related to the shadowing type of satellite channels, and the values of channel shadowing parameters b_k, m_k and Ω_k are increased successively in HS and AS scenarios. Moreover, by comparing the outage probability for the HS and AS scenarios, we can observe that the AS case yields better outage performance than the HS case. The reason for this phenomenon is that the line-of-sight signal component in the received signal is not obscured and the multipath component has high average power in average shadowing condition, so the outage event does not occur [33].

Fig. 4 illustrates the impact of different angles between the terrestrial users and the antenna beam center on the outage performance, where $\psi = \psi_1 = \psi_2 = \psi_3 = \{0.1°, 0.6°, 0.9°\}$ and the satellite channels undergo AS. With ψ increases, the outage probabilities for the users increase, which is intuitional. This indicates that with the increase of ψ, the terrestrial users approach the edge of satellite coverage areas.

Fig. 5(a) illustrates the system throughput versus the transmit SNR with different levels of residual interference signal in delay-limited transmission mode. In this case, we set the level of residual interference $\varpi = \{0, 0.1, 0.2\}$, and the system throughput of orthogonal user is chosen to be the benchmark denoted by black solid curves. As can be seen from Fig. 5(a), the sum throughput of NOMA users with imperfect/perfect SIC is lower than that of conventional orthogonal user in low SNR region. This is due to the fact that the NOMA based satellite-terrestrial system has high outage probability when the transmit SNR is below 15 dB. In addition, we can find that the sum throughput of NOMA users decreases as the level of residual interference increases in low SNR region, and the sum throughput of perfect SIC and imperfect SIC are almost equal if the transmit SNR is greater than 25 dB. Fig. 5(b) shows the influences of the transmit SNR and various length of training symbols on the sum throughput of proposed system. Apparently, system throughput increases as the transmit SNR increases. Further, throughput performance declines significantly when the value of training symbol decreases from 5 to 1 in middle and low SNR region. Therefore, it is

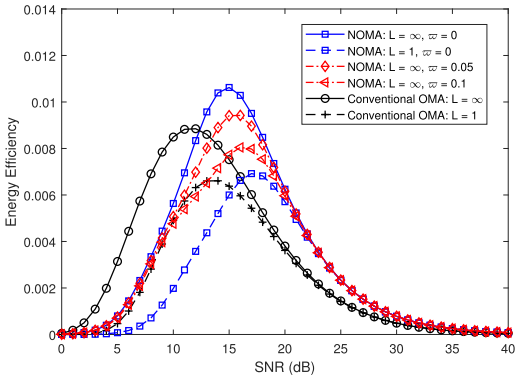

FIGURE 7. Energy efficiency versus the transmit SNR in delay-limited transmission mode.

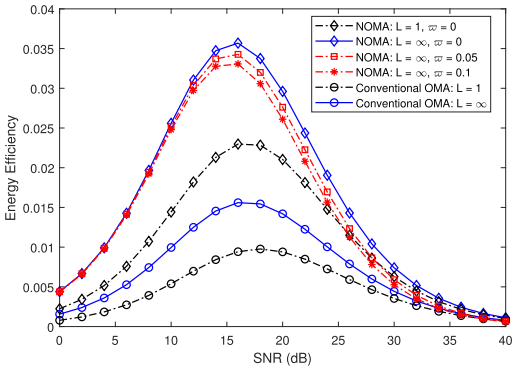

FIGURE 8. Energy efficiency versus the transmit SNR in delay-tolerant transmission mode.

important to consider the impact of L when designing practical NOMA based satellite-terrestrial system.

Fig. 6(a) shows the ergodic rates versus the transmit SNR with different levels of residual interference, where $\varpi = \{0, 0.01, 0.02, 0.03\}$. We can observe that the sum rate of the proposed system decreases as the level of residual interference ϖ increases, and is even lower than that of conventional OMA once ϖ goes beyond a specific value. This indicates that in the presence of residual interference, the ergodic rate is sensitive to ϖ. In addition, it is shown in Fig. 6(a) that the NOMA users with perfect SIC are capable of outperforming the orthogonal user on the sum rate. The reason for this phenomenon is that NOMA provides services for multiple users in the same physical resource, which improves user fairness and again validates the conclusions consistent with Fig. 1. In addition, it can also be seen that the sum rate in AS mode is superior to that in HS mode under the same conditions. In Fig. 6(b), the ergodic rates of the considered system are plotted for imperfect CSI, $L = 1, 2, 5$, and perfect CSI ($L = \infty$). In this example, we fix the level of residual interference as $\varpi = 0$. Apparently, as the value of the training symbol decreases, the sum rate gradually decreases. Therefore, it is important to consider the effect of imperfect CSI when designing practical systems, and the performance of ergodic rates can be improved by increasing the length of training symbols. Moreover, as shown in figure, the sum rate of the proposed NOMA based satellite-terrestrial network always outperforms the orthogonal multiple access network, which indicates the superiority of the NOMA strategy.

Fig. 7 illustrates the effects of the transmit SNR, the level of residual interference ϖ and channel estimation error on the energy efficiency of the proposed system in delay-limited transmission mode, which can be obtained from (27). In this example, we set the power amplification factor $\varepsilon = 2$, and $P_L = 50$ W [10]. As we can see from Fig. 7, the energy efficiency for NOMA system and OMA system decrease with the increase of channel estimation error (the decrease of the length of training symbol). Further, the energy efficiency of NOMA schemes increases gradually with the increase of SNR, and reaches the maximum at a certain point. When ϖ increases from 0 to 0.1, the energy efficiency of NOMA schemes significantly decreases, and the point corresponding to the maximum energy efficiency in the figure moves to the right. Meanwhile, it can be observed that the energy efficiency of the proposed system is inferior to the conventional OMA schemes in the low SNR region. This is because NOMA schemes can not achieve larger throughput than that of OMA schemes in this SNR region, which has been confirmed in Fig. 5.

Fig. 8 shows the energy efficiency versus the transmit SNR with different levels of residual interference and different training symbol lengths in delay-tolerant transmission mode, where $\varpi = \{0, 0.05, 0.1\}$ and $L = \{0, \infty\}$. Here, as in Fig. 7, we assume $\varepsilon = 2$, and $P_L = 50$ W. As illustrated, NOMA schemes with imperfect CSI and SIC can acquire better energy efficiency performance than that of conventional OMA schemes in this transmission mode. Another observation is that the energy efficiency performance is closely related to the level of residual interference, and decreases with the increase of ϖ. This is due to the fact that the ergodic rate achieved by the NOMA users decreases when ϖ increases, as analyzed in Fig. 6(a). This observation indicates that the introduction of NOMA technology into satellite communications can effectively improve the system energy efficiency and reduce the loss of satellite power modules. In addition, it is of great significance to design a reasonable SIC strategy for the proposed NOMA based satellite-terrestrial system in the application scenario.

VII. CONCLUSION

In this paper, we have investigated the NOMA based satellite-terrestrial system with imperfect CSI and imperfect SIC under Shadowed-Rician fading channel. The performance of the NOMA based satellite-terrestrial system is characterized. The closed-form expressions for the exact and asymptotic outage probabilities are derived, and the effect of channel parameters on the performance of the proposed system is also considered. Our analysis showcased that the outage performance decreases to different degrees due to the influence of imperfect CSI and the residual interference signals. The performance NOMA scheme is capable of outperforming conventional orthogonal scheme on the outage

probability. Furthermore, the ergodic sum rate and system throughput expressions are obtained. The simulation results verify the accuracy of the analysis results and the advantages of NOMA scheme. Finally, we discuss the system energy efficiency in delay-limited and delay-tolerant transmission modes. It can be found that the energy efficiency is very sensitive to the level of residual interference, and the study on residual interference can provide guidance for SIC design in practical application scenarios.

APPENDIX
PROOF OF EQUATION (23)

First, by combining (20), (21) and (22), Φ_1 can be calculated as

$$\begin{aligned}\Phi_1 &= \frac{1}{\ln 2}\int_0^{\infty} \ln\left(1+\Lambda_k X_k\right) f_{X_k^*}(x)\,dx \\ &= \frac{\Xi_k}{\Gamma(m_k)\ln 2}\sum_{r=0}^{N-k}\binom{N-k}{r}(-1)^r\,\alpha_k^{k+r} \\ &\quad\times\int_0^{\infty} x^{k+r-1}e^{-\beta_k x}G_{2,2}^{1,2}\left[\Lambda_k x\,\middle|\,\begin{matrix}1, & 1\\ 1, & 0\end{matrix}\right] \\ &\quad\times G_{1,2}^{1,1}\left[-\delta_k x\,\middle|\,\begin{matrix}1-m_k\\ 0, \quad 0\end{matrix}\right]dx \\ &\overset{\text{(iii)}}{=} \frac{\Xi_k}{\Gamma(m_k)\ln 2}\sum_{r=0}^{N-k}\binom{N-k}{r}(-1)^r\,\alpha_k^{k+r}\beta_k^{-k-s} \\ &\quad\times G_{1,[1:2],0,[2:2]}^{1,1,2,1,1}\left[\begin{matrix}\frac{-\delta_k}{\beta_k}\\ \\ \frac{\Lambda_k}{\beta_k}\end{matrix}\,\middle|\,\begin{matrix}(k+r,1)\\ (1-m_k);(1,1)\\ -\\ (0,0);(1,0)\end{matrix}\right]\end{aligned} \tag{A.1}$$

where the step (iii) follows [34, eq.(2.6.2)].

The proof is completed.

REFERENCES

[1] Y. Saito, Y. Kishiyama, A. Benjebbour, T. Nakamura, A. Li, and K. Higuchi, "Non-orthogonal multiple access (NOMA) for cellular future radio access," in *Proc. IEEE 77th Veh. Technol. Conf. (VTC Spring)*, Jun. 2013, pp. 1–5.

[2] Z. Ding, Z. Yang, P. Fan, and H. V. Poor, "On the performance of non-orthogonal multiple access in 5G systems with randomly deployed users," *IEEE Signal Process. Lett.*, vol. 21, no. 12, pp. 1501–1505, Dec. 2014.

[3] Z. Ding, P. Fan, and H. V. Poor, "Impact of user pairing on 5G nonorthogonal multiple-access downlink transmissions," *IEEE Trans. Veh. Technol.*, vol. 65, no. 8, pp. 6010–6023, Aug. 2016.

[4] Z. Ding, Y. Liu, J. Choi, Q. Sun, M. Elkashlan, I. Chih-Lin, and H. V. Poor, "Application of non-orthogonal multiple access in LTE and 5G networks," *IEEE Commun. Mag.*, vol. 55, no. 2, pp. 185–191, Feb. 2017.

[5] X. Yue, Y. Liu, S. Kang, A. Nallanathan, and Z. Ding, "Exploiting full/half-duplex user relaying in NOMA systems," *IEEE Trans. Commun.*, vol. 66, no. 2, pp. 560–575, Feb. 2018.

[6] X. Zhu, C. Jiang, L. Kuang, N. Ge, and J. Lu, "Non-orthogonal multiple access based integrated terrestrial-satellite networks," *IEEE J. Sel. Areas Commun.*, vol. 35, no. 10, pp. 2253–2267, Oct. 2017.

[7] Y. Lin, S. Wang, X. Bu, C. Xing, and J. An, "NOMA-based calibration for large-scale spaceborne antenna arrays," *IEEE Trans. Veh. Technol.*, vol. 67, no. 3, pp. 2231–2242, Mar. 2018.

[8] A. I. Perez-Neira, M. Caus, and M. A. Vazquez, "Non-orthogonal transmission techniques for multibeam satellite systems," *IEEE Commun. Mag.*, vol. 57, no. 12, pp. 58–63, Dec. 2019.

[9] T. Qi, W. Feng, and Y. Wang, "Outage performance of non-orthogonal multiple access based unmanned aerial vehicles satellite networks," *China Commun.*, vol. 15, no. 5, pp. 1–8, May 2018.

[10] X. Yan, H. Xiao, C.-X. Wang, K. An, A. T. Chronopoulos, and G. Zheng, "Performance analysis of NOMA-based land mobile satellite networks," *IEEE Access*, vol. 6, pp. 31327–31339, 2018.

[11] M. Jia, Q. Gao, Q. Guo, X. Gu, and X. Shen, "Power multiplexing NOMA and bandwidth compression for satellite-terrestrial networks," *IEEE Trans. Veh. Technol.*, vol. 68, no. 11, pp. 11107–11117, Nov. 2019.

[12] Z. Lin, M. Lin, J.-B. Wang, T. de Cola, and J. Wang, "Joint beamforming and power allocation for satellite-terrestrial integrated networks with non-orthogonal multiple access," *IEEE J. Sel. Topics Signal Process.*, vol. 13, no. 3, pp. 657–670, Jun. 2019.

[13] X. Zhang, B. Zhang, K. An, Z. Chen, S. Xie, H. Wang, L. Wang, and D. Guo, "Outage performance of NOMA-based cognitive hybrid satellite-terrestrial overlay networks by amplify-and-forward protocols," *IEEE Access*, vol. 7, pp. 85372–85381, 2019.

[14] V. Singh, P. K. Upadhyay, and M. Lin, "On the performance of NOMA-assisted overlay multiuser cognitive satellite-terrestrial networks," *IEEE Wireless Commun. Lett.*, vol. 9, no. 5, pp. 638–642, May 2020.

[15] Z. Yin, M. Jia, W. Wang, N. Cheng, F. Lyu, Q. Guo, and X. Shen, "Secrecy rate analysis of satellite communications with frequency domain NOMA," *IEEE Trans. Veh. Technol.*, vol. 68, no. 12, pp. 11847–11858, Dec. 2019.

[16] X. Wu, M. Lin, H. Kong, Q. Huang, J.-Y. Wang, and P. K. Upadhyay, "Outage performance for multiuser threshold-based DF satellite relaying," *IEEE Access*, vol. 7, pp. 103142–103152, 2019.

[17] Q. Zhang, K. An, X. Yan, and T. Liang, "Coexistence and performance limits for the cognitive broadband satellite system and mmWave cellular network," *IEEE Access*, vol. 8, pp. 51905–51917, 2020.

[18] X. Li, M. Liu, C. Deng, D. Zhang, X.-C. Gao, K. M. Rabie, and R. Kharel, "Joint effects of residual hardware impairments and channel estimation errors on SWIPT assisted cooperative NOMA networks," *IEEE Access*, vol. 7, pp. 135499–135513, 2019.

[19] S. Xie, B. Zhang, D. Guo, and W. Ma, "Outage performance of NOMA-based integrated satellite-terrestrial networks with imperfect CSI," *Electron. Lett.*, vol. 55, no. 14, pp. 793–795, Jul. 2019.

[20] X. Yan, K. An, C.-X. Wang, W.-P. Zhu, Y. Li, and Z. Feng, "Genetic algorithm optimized support vector machine in NOMA-based satellite networks with imperfect CSI," in *Proc. IEEE Int. Conf. Acoust., Speech Signal Process. (ICASSP)*, May 2020, pp. 8817–8821.

[21] X. Yue, Z. Qin, Y. Liu, S. Kang, and Y. Chen, "A unified framework for non-orthogonal multiple access," *IEEE Trans. Commun.*, vol. 66, no. 11, pp. 5346–5359, Nov. 2018.

[22] X. Li, M. Liu, C. Deng, P. T. Mathiopoulos, Z. Ding, and Y. Liu, "Full-duplex cooperative NOMA relaying systems with I/Q imbalance and imperfect SIC," *IEEE Wireless Commun. Lett.*, vol. 9, no. 1, pp. 17–20, Jan. 2020.

[23] G. Im and J. H. Lee, "Outage probability for cooperative NOMA systems with imperfect SIC in cognitive radio networks," *IEEE Commun. Lett.*, vol. 23, no. 4, pp. 692–695, Apr. 2019.

[24] X. Yue, Y. Liu, Y. Yao, T. Li, X. Li, R. Liu, and A. Nallanathan, "Outage behaviors of NOMA-based satellite network over Shadowed-Rician fading channels," *IEEE Trans. Veh. Technol.*, vol. 69, no. 6, pp. 6818–6821, Jun. 2020.

[25] G. Zheng, S. Chatzinotas, and B. Ottersten, "Generic optimization of linear precoding in multibeam satellite systems," *IEEE Trans. Wireless Commun.*, vol. 11, no. 6, pp. 2308–2320, Jun. 2012.

[26] A. Abdi, W. C. Lau, M. Alouini, and M. Kaveh, "A new simple model for land mobile satellite channels: First- and second-order statistics," *IEEE Trans. Wireless Commun.*, vol. 2, no. 3, pp. 519–528, May 2003.

[27] I. S. Gradshteyn and I. M. Ryzhik, *Table of Integrals, Series and Products*, 6th ed. New York, NY, USA: Academic, 2000.

[28] H. A. David and H. N. Nagaraja, *Order Statistics*, 3rd ed. New York, NY, USA: Wiley, 2003.

[29] P. K. Sharma, P. K. Upadhyay, D. B. da Costa, P. S. Bithas, and A. G. Kanatas, "Performance analysis of overlay spectrum sharing in hybrid satellite-terrestrial systems with secondary network selection," *IEEE Trans. Wireless Commun.*, vol. 16, no. 10, pp. 6586–6601, Oct. 2017.

[30] V. S. Adamchik and O. I. Marichev, "The algorithm for calculating integrals of hypergeometric type functions and its realization in reduce system," in *Proc. ISSAC*. New York, NY, USA: Association for Computing Machinery, 1990, pp. 212–224.

[31] R. P. Agrawal, "On certain transformation formulae and Meijer's G-function of two variables," *Indian J. Pure Appl. Math.*, vol. 1, no. 4, pp. 537–551, Sep. 1970.
[32] X. Yue, Y. Liu, S. Kang, A. Nallanathan, and Y. Chen, "Modeling and analysis of two-way relay non-orthogonal multiple access systems," *IEEE Trans. Commun.*, vol. 66, no. 9, pp. 3784–3796, Sep. 2018.
[33] E. Lutz, D. Cygan, M. Dippold, F. Dolainsky, and W. Papke, "The land mobile satellite communication channel-recording, statistics, and channel model," *IEEE Trans. Veh. Technol.*, vol. 40, no. 2, pp. 375–386, May 1991.
[34] A. Mathai and R. Saxena, *The H-Function With Applications in Statistics and Other Disciplines*. New York, NY, USA: Wiley, 1978.

JINLONG ZHAO received the M.Sc. degree from the School of Computer and Communication, Lanzhou University of Technology, Lanzhou, China, in 2013. He is currently pursuing the Ph.D. degree in communication and information systems with the School of Electronic and Information Engineering, Beihang University.

His current research interests include cooperative networks, non-orthogonal multiple access, and satellite-terrestrial communications.

XINWEI YUE (Member, IEEE) received the Ph.D. degree in communication and information system from Beihang University (BUAA), Beijing, in 2018. He is currently an Associate Professor with the School of Information and Communication Engineering, Beijing Information Science and Technology University (BISTU), Beijing.

His research interests include 5G/6G networks, wireless communications theory, non-orthogonal multiple access, cooperative networks, and physical layer security.

SHAOLI KANG was a Project Manager with the China Academy of Telecommunications Technology (CATT), focusing on the Research and Development of TD-SCDMA, from 2000 to 2005. She was with the Communication Center of System Research, University of Surrey, as a Research Fellow, doing research on projects from EPSRC and OFCOM, and leading the Antenna and Propagation Club. Since 2007, she has been with CATT, as the Vice-Chief Engineer of TDD Research and Development product line, focusing on speeding up the standard and industrial progress of TDD technology. Since 2011, she has been with the Wireless Innovation Center, CATT, as the Head Expert leading the 5G research, where she is currently the Head Expert of 5G Standardization. She has authored over 20 articles. She has applied over 50 patents.

WANWEI TANG received the B.E. degree from Dalian Polytechnic University, in 2006, the M.S. degree from Dalian Maritime University, in 2008, and the Ph.D. degree from Beihang University, in 2019. Since 2018, he has been an Assistant Professor with the Intelligence and Information Engineering College, Tangshan University.

His research interests include 5G wireless networks, wireless communications theory, wireless communications systems, detection algorithm, and cooperative networks.